C–C σ-Bond Oxidative Addition and Hydrofunctionalization by a Macrocycle-Supported Diiron Complex

Tianchang Liu, Ryan P. Murphy, Patrick J. Carroll, Michael R. Gau and Neil C. Tomson

Roy and Diana Vagelos Laboratories, Department of Chemistry, University of Pennsylvania, Philadelphia, Pennsylvania 19104, United States

ABSTRACT: This report describes the first examples of unassisted C(*sp*)–C(sp^2) and C(*sp*)–C(sp^3) bond oxidative addition reactions to give thermodynamically favorable products. Treatment of a diiron complex supported by a geometrically and electronically flexible macrocyclic ligand, (^{3}PDI$_2$)Fe$_2$(μ-N$_2$)(PPh$_3$)$_2$ (**[Fe$_2$N$_2$]^0**), with stoichiometric amounts of various 4,4'-disubstituted diphenylacetylenes (Ar^X–C≡C–Ar^X; X = OMe, H, F, CF$_3$) yielded C(*sp*)–C(sp^2) bond oxidative addition products. When Ph–C≡C–R substrates were used as substrates (R = Me, Et, ^{i}Pr, ^{t}Bu), products of either C(*sp*)–C(sp^2) or C(*sp*)–C(sp^3) bond activation were obtained, with the less sterically encumbering alkynes exclusively undergoing C(*sp*)–C(sp^3) bond activation. Treatment of the C–C activation species with either H$_2$ or HBpin were found to form products of C–C σ-bond hydrofunctionalization. In both the hydrogenation and hydroboration schemes, the diiron species was observed to return to **[Fe$_2$N$_2$]^0**, thereby completing synthetic cycles for C–C σ-bond functionalization.

The selective cleavage and functionalization of C−C σ-bonds are highly attractive, yet challenging, chemical transformations of interest for targets as varied as complex molecule synthesis, biomass conversion, and petrochemical processing.[1-5] The activation of these bonds is, however, generally disfavored compared to C–H bond activation due to several factors, including the relative inaccessibility of C–C σ* orbitals and the lower driving force for C–C activation at a transition metal center. Several methods are known to assist C–C bond cleavage (Figure 1, top). These include anchimeric and chelation effects,[6] the formation of conjugated systems on activation,[6] β-carbon elimination,[6-7] and, most notably, the use of strained 3- and 4-membered rings that are predisposed to undergo activation due to internal ring strain.[8-12] However, the *unassisted* oxidative addition of strong C−C σ-bonds continues to pose a challenge as a result of unfavorable kinetic and thermodynamic profiles.[13-15] Considering the prevalence of C–C σ-bonds, the development of methods for performing unassisted C–C σ-bond activation, ideally with regiochemical control under mild conditions, remains a topic of significant academic and industrial interest.

Alkynyl-aryl connections are particularly resistant to unassisted activation and functionalization. While a few systems are known that generate products of C(*sp*)–C(sp^2) bond functionalization, this chemistry uses precious metals and occurs through mechanisms that do not involve direct C(*sp*)–C(sp^2) bond activation.[16-18] The direct oxidative addition of C(*sp*)–C(sp^2) bonds has only been reported at a family of (*cis*-L$_2$)Pt^0(η^2-alkyne) (L = phosphine, amine) complexes (Figure 1, middle).[15, 19-22] These require the use of photochemical conditions to access endergonic Pt^{II} products that, in turn, thermally revert to the Pt^0(η^2-alkyne) starting materials. Computational studies have been used to support the proposal that these systems undergo C–C bond cleavage following initial photoisomerization to a Pt-arene adduct.[23] The photochemically driven formation of an arene adduct is then thought to explain the exclusive cleavage of C(*sp*)–C(sp^2) bonds when in the presence of weaker C(*sp*)–C(sp^3) σ-bonds. What's more, no examples have been provided in the literature of functionalization of the Pt-based oxidative addition products.

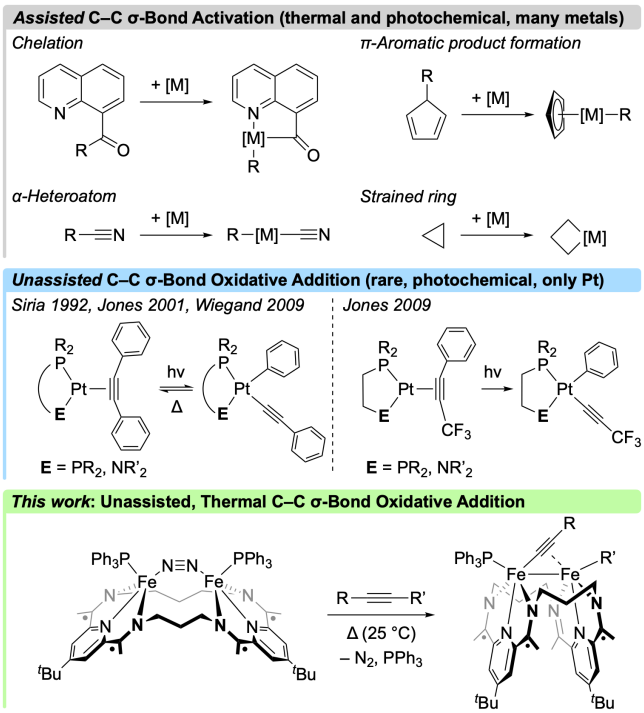

Figure 1. Overview of strategies for *assisted* and *unassisted* C–C σ-bond activation by transition metal complexes.

Herein, we disclose our findings that a macrocycle-supported diiron complex is competent for direct C(*sp*)−C(sp^2) and C(*sp*)−C(sp^3) bond oxidative addition reactions under thermal conditions (Figure 1, bottom). The C–C activated products are then shown to be intermediates in synthetic cycle for C–C σ-bond hydrofunctionalization schemes.

The work described here makes use of a diiron bridging dinitrogen complex (^{3}PDI$_2$)Fe$_2$(μ-N$_2$)(PPh$_3$)$_2$ (**[Fe$_2$N$_2$]^0**) supported by a pyridyldiimine (PDI)-based macrocyclic ligand, ^{3}PDI$_2$.[24] This species is composed of two Fe^{II} centers bound within a ^{3}PDI$_2$ ligand that contains four electrons' worth of electron density in its π*-manifold, as determined by characteristic bond lengths in the ligand backbone.[25-26] Treatment of a THF solution of **[Fe$_2$N$_2$]^0** with 1.0 equiv of diphenylacetylene at room temperature results in a gradual color change from red to green over 16 h that corresponds to the formation of a C(*sp*)–C(*sp*^{2}) bond oxidative addition product, (^{3}PDI$_2$)Fe$_2$(μ-C≡CPh)(Ph)(PPh$_3$) (**1^H**, Scheme 1). ^{1}H and ^{31}P{^{1}H} NMR spectra of the reaction mixture revealed complete consumption of the starting material and clean formation of **1^H** and free PPh$_3$. Two distinct sets of signals were observed that encompass the characteristic pyridyl, imine-methyl and *tert*-butyl protons of the PDI ligand fragments of **1^H**, indicative of a diamagnetic product with a desymmetrized ligand scaffold. One ^{31}P{^{1}H} NMR spectral resonance (60.9 ppm) was observed in addition to that of free PPh$_3$, indicating that one PPh$_3$ remained bound to a metal center.

Scheme 1. Synthesis and proposed reaction pathway for the formation of 1^X from [Fe$_2$N$_2$]^0 and diphenylacetylenes.

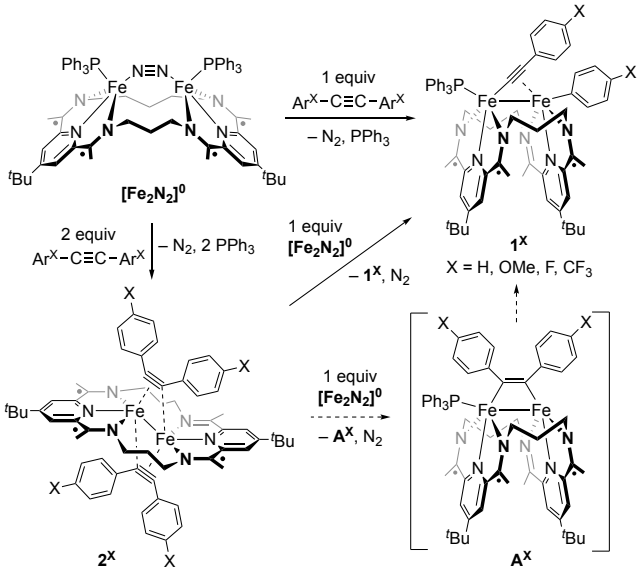

A crystallographic analysis of **1^H** revealed a C_s-symmetric species (Figure 2), in which a μ-κ^1:η^2-phenylacetylide ligand spanned two metals and a terminal phenyl ligand was bound to a phosphine-free Fe center (Fe2). The C≡C bond length of 1.272(9) Å is elongated compared to free diphenylacetylene (1.198 Å), consistent with a modest amount of π-backbonding *via* the η^2 interaction with Fe2. The ligand adopts a "folded" conformation, which provides for an Fe–Fe distance of 2.765(1) Å that is in the range of other known Fe–Fe single bonds. Along with the change in geometry, the crystallographic data were consistent with a ^{3}PDI$_2$ ligand that contains three electrons' worth of electron density in its π* system, indicating that **1^H** contains a net charge distribution of (^{3}PDI$_2$)$^{3-}$:(Fe$_2$)$^{5+}$ within a set of covalent Fe–PDI and Fe–Fe interactions. As observed by Chirik and co-workers for the Fe-mediated oxidative addition of a strained C(*sp*^{2})–C(*sp*^{2}) bond,[27] the present system appears to use both metal- and ligand-based electron density during the 2e$^-$ oxidative addition process.

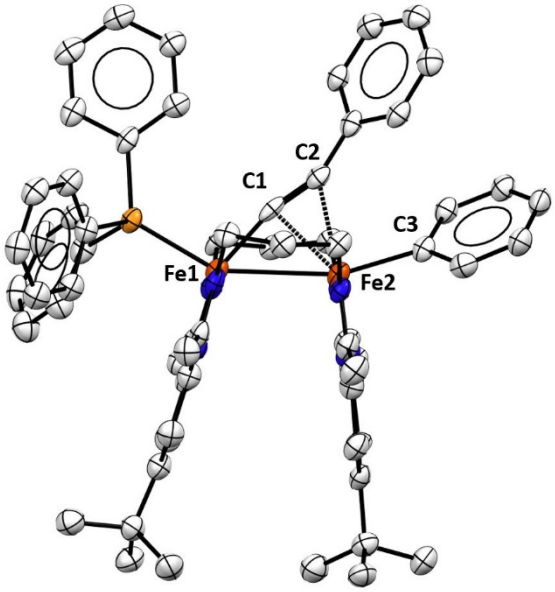

Figure 2. Crystal structure of **1^H**. Hydrogen atoms are omitted for clarity. Selected bond length: Fe1–Fe2 = 2.765(1) Å, Fe1–C1 = 1.872(6) Å, Fe2–C1 = 2.115(5) Å, Fe2–C2 = 2.257(6) Å, Fe2–C3 = 2.014(6) Å.

Various 4,4'-disubstituted diphenylacetylenes (Ar^{X}CCAr^X; X = OMe, F, CF$_3$) were similarly found to undergo oxidative addition at their C(*sp*)–C(*sp*^{2}) σ-bonds to yield products (**1^X**, Scheme 1, see Supporting Information) that are isostructural to **1^H**. The relative rates of the reactions to form **1^X** indicated that the electron-rich derivatives react faster than the electron-poor ones (X = OMe >> CF$_3$; see Supporting Information). Monitoring the reaction by ^{1}H NMR spectroscopy revealed, in all cases, the rapid formation of a diamagnetic intermediate, **2^X**, with a 2:1 alkyne:^{3}PDI$_2$ stoichiometry that converted to **1^X** over time. Use of the electron-deficient alkyne Ar^{CF3}CCAr^{CF3} led to the successful isolation and structural characterization of **2^{CF3}** as a diiron dialkyne adduct (^{3}PDI$_2$)Fe$_2$[μ-(Ar^{CF3}CCAr^{CF3})]$_2$ (Scheme 1), in which the ligand adopts an "unfolded" conformation and two alkynyl units are bound in μ-η^1:η^2 binding modes to either side of the macrocycle. While thermolysis of **2^{CF3}** in the presence of added PPh$_3$ produced a mixture of unidentified products, treatment of **2^{CF3}** with **[Fe$_2$N$_2$]^0** cleanly formed 2 equiv. of the C–C activation product **1^{CF3}** in high yield (92 %). No intermediate was observed via ^{1}H and ^{31}P{^{1}H} NMR spectroscopy during this latter conversion. These data are consistent with an energy landscape that involves the kinetically facile formation of **2^X**, which undergoes reversible, endergonic loss of alkyne to generate a species that is able to cleave a C–C bond to form **1^X**. A transient mono-alkyne adduct, (^{3}PDI$_2$)Fe$_2$[μ-(Ar^{X}CCAr^X)](PPh$_3$) (**A^X**, Scheme 1), is thus proposed as an immediate precursor to C–C bond cleavage.

Carrying out the reaction of **[Fe$_2$N$_2$]^0** with 1.0 equiv. of diphenylacetylene in the dark did not slow the reaction rate, indicating that light is not participating in the C–C bond activation process. Considering this divergence from the photochemical Pt chemistry for unassisted C–C σ-bond activation described above, we investigated the reactivity of **[Fe$_2$N$_2$]^0** towards a series of asymmetric alkynes. Treatment of **[Fe$_2$N$_2$]^0** with PhCCMe gradually formed the product of C(*sp*)–C(*sp*^{3}) bond cleavage, (^{3}PDI$_2$)Fe$_2$(C≡CPh)(Me)(PPh$_3$) (**3^{Me}**, Scheme 2), in good spectroscopic yield. The ^{1}H NMR spectrum for this product featured a characteristically upfield-

shifted resonance for the Fe-bound methyl group protons at 0.16 ppm (C_6D_6, 298 K). Treatment of **$[Fe_2N_2]^0$** with PhCCEt similarly generated a product of C(*sp*)–C(sp^3) bond cleavage, (^{3}PDI$_2$)Fe$_2$(C≡CPh)(Et)(PPh$_3$) (**3^{Et}**); however, use of PhCC^{i}Pr and PhCC^{t}Bu resulted in the exclusive formation of the C(*sp*)–C(sp^2) bond cleavage products (^{3}PDI$_2$)Fe$_2$(C≡C^{i}Pr)(Ph)(PPh$_3$) (**4^{iPr}**) and (^{3}PDI$_2$)Fe$_2$(C≡C^{t}Bu)(Ph)(PPh$_3$) (**4^{tBu}**, Scheme 2). While detailed mechanistic studies are ongoing, it appears both that the formation of an Fe–arene interaction is not needed as a direct precursor to C–C activation and that C(*sp*)–C(sp^3) activation may be thermodynamically preferred over C(*sp*)–C(sp^2) bond activation; these points are supported by the results of preliminary density functional theory (DFT) calculations (see below and the Supporting Information).

Scheme 2. Selective C–C bond activation with aryl-alkyl acetylenes by $[Fe_2N_2]^0$.

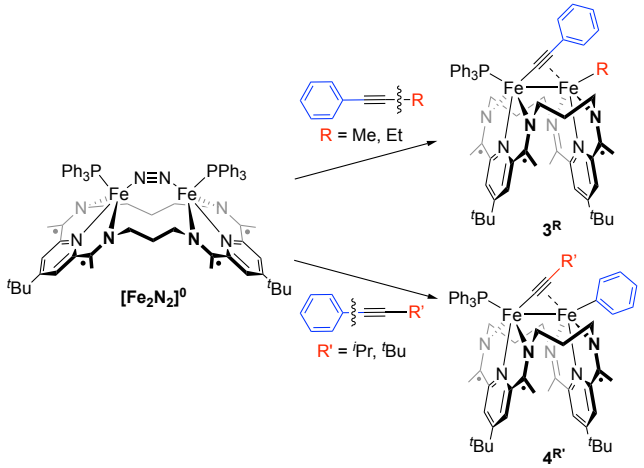

A preliminary computational investigation into the reaction coordinate of C–C bond activation was performed using a truncated version of the proposed monoalkyne adduct, (^{3}PDI$_2$')Fe$_2$(μ-PhCCPh)(PMe$_3$) (**A'**, Figure 3, see Supporting Information). DFT calculations predicted this species to display an alkynyl unit that bridges symmetrically between the two metal centers (d_{FeFe} = 2.59 Å) in a form that may be best represented as a doubly deprotonated olefin (d_{CC} = 1.36 Å; d_{FeC} = 1.95, 1.96 Å). A C–C bond cleavage transition state structure was identified at +11.4 kcal/mol, at which point the alkynyl unit "docks" at Fe1, forming an η^2-adduct with a shortened C–C distance (1.30 Å). This docking interaction places a C(*sp*)–C(sp^2) bond in position to generate a 3-membered ring at Fe2; movement within this 3-membered ring provides most of the motion through the transition state. Inspection of the IAO-IBO orbitals for **TS$_{A'B'}$**, revealed mixing of a {d_{xz} + PDI-π*} orbital on Fe2 with the C(*sp*)–C(sp^2) σ^* orbital (Figure 3, inset), highlighting the capacity of both the metal and the redox-active PDI ligand to engage in the C–C bond cleavage process. Following activation, the structure relaxes to a species that accommodates both the aryl and acetylide units at Fe2 (**B'**). A low-energy isomerization process (**TS$_{B'C'}$**) inverts the orientation of the acetylide to generate **C'**, which displays a satisfactory model of the crystallographically characterized complex **1^H**.[28] Notably, the Fe–Fe distance was found to expand during this transformation, first to 2.69 Å in **TS$_{A'B'}$**, then 2.73 Å in the calculated structure for **C'**. The ability of the dinuclear core to accommodate various binding modes both during and after C–C bond cleavage (see Supporting Information) appears to impact both the kinetics and the thermodynamics of this transformation.

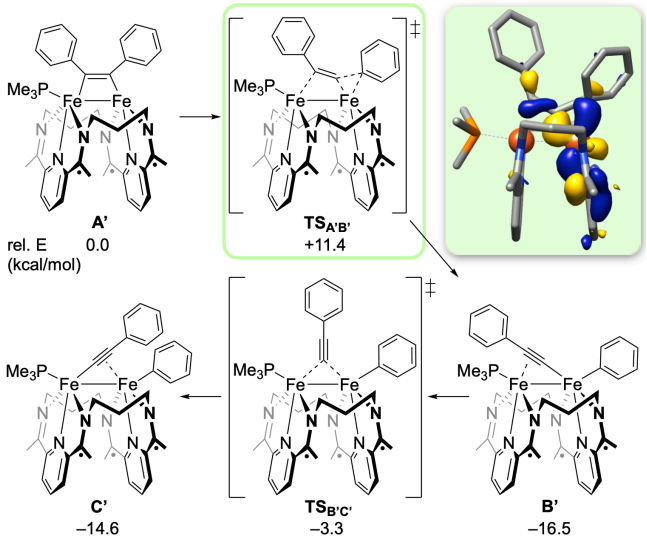

Figure 3. DFT-calculated reaction coordinate for C–C σ-bond oxidative addition. *Inset:* Depiction of key IAO-IBO orbital in **TS$_{A'B'}$**, that facilitates C–C bond cleavage.

We next investigated the reactivity of the C–C activation products for net hydrofunctionalization of the C–C σ-bond. Treatment of C_6D_6/THF-d_8 solutions of **1^X**, **3^R**, or **4$^{R'}$** with 1 atm of H_2 resulted in all cases in a gradual color change from green to brown. NMR spectroscopic studies revealed formation of the products of both net C–C σ-bond hydrogenation and hydrogenation of the alkynyl unsaturation, generating ethylarene/ethylalkane and arene/alkane products in good yields (Scheme 3). Monitoring these reactions by NMR spectroscopy revealed the regeneration of **$[Fe_2N_2]^0$**, which gave way to a diamagnetic diiron dihydride complex (^{3}PDI$_2$)Fe$_2$(μ-H)$_2$(PPh$_3$)$_2$ (**$[Fe_2H_2]^0$**, Figure S8 in Supporting Information). The independent treatment of **$[Fe_2N_2]^0$** with H_2 was found to form **$[Fe_2H_2]^0$** in quantitative spectroscopic yield (Scheme 3), consistent with the view that the formation of **$[Fe_2H_2]^0$** results from H_2 activation by **$[Fe_2N_2]^0$**.

In a related attempt to functionalize a product of C–C σ-bond activation, we treated **3^{Me}** with 2.0 equiv. of HBpin at room temperature. Doing so formed *E*-PhCH=CHBpin, CH_3Bpin and CH_4, along with the diiron species **$[Fe_2N_2]^0$**, in modest yields (Scheme 3). These products constitute the net hydroboration of a C–C σ-bond and the semihydroboration of the alkynyl unit. Unidentified products were present in the reaction mixture, along with *ca*. 0.3 equiv of unreacted HBpin, but return of the diiron species to **$[Fe_2N_2]^0$** indicates that this system, like the hydrogenation chemistry described above, is able to engage in a synthetic cycle for C–C σ-bond functionalization. We note that HBpin was found to be unreactive toward **$[Fe_2N_2]^0$** under the reaction conditions, suggesting that the system may be rendered fully catalytic; however, initial attempts to do so solely yielded vinylboronic esters without C–C σ-bond activation (*Z*-PhC(Bpin)=C(H)Me and *Z*-PhC(H)=C(Bpin)Me in a 73:27 ratio). More work will need to be done to determine the mechanisms of the hydrofunctionalization transformations and to develop strategies for performing them under catalytic conditions.

Scheme 3. Hydrogenation and hydroboration reactivity with C−C activation complexes.

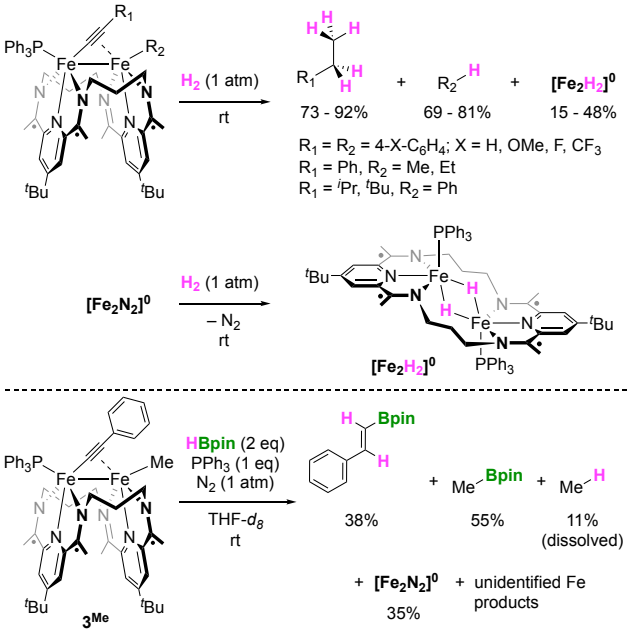

This report constitutes the first examples of unassisted oxidative addition of C(*sp*)–C(sp^2) and C(*sp*)–C(sp^3) σ-bonds to give thermodynamically favorable products. These reactions were mediated by a macrocycle-supported diiron complex, whose geometry was found to change significantly through the course of the reaction, from an "arched" ligand geometry for the N_2-coordinated starting material, to an "unfolded" ligand in a dialkyne kinetic product and a "folded" ligand geometry following C–C bond oxidative addition. For the alkynes with mixed aryl-alkyl substitution patterns, regioselective C(*sp*)−C(sp^2)/C(sp^3) bond activations were achieved, depending on the identity of alkyl group. Stepwise catalytic σ-bond hydrofunctionalizations of C(*sp*)−C(sp^2)/C(sp^3) bonds were realized on treatment of the oxidative addition products with H_2 or HBpin to generate the corresponding hydrogenation and hydroboration products. Further investigations are underway to elaborate the scope of C–C bond hydrofunctionalization chemistry and to understand the mechanism by which the present diiron system mediates the reactivity described above.

ASSOCIATED CONTENT

Supporting Information.
The Supporting Information is available free of charge at xxxx.

Experimental section, crystallographic data, NMR spectra, computational details (PDF)

AUTHOR INFORMATION

Corresponding Author

Neil C. Tomson − Roy and Diana Vagelos Laboratories, Department of Chemistry, University of Pennsylvania, Philadelphia, Pennsylvania 19104, United States; orcid.org/ 0000-0001-9131-1039; Phone: +1 (215) 898-6208; Email: tomson@upenn.edu

Authors

Tianchang Liu − orcid.org/ 0000-0003-0629-6167

Ryan P. Murphy − orcid.org/ 0000-0002-0700-2880

Patrick J. Carroll − orcid.org/ 0000-0002-8142-7211

Michael R. Gau − orcid.org/ 0000-0002-4790-6980

ACKNOWLEDGMENT

We thank the National Science Foundation (CHE-1945265) and the University of Pennsylvania for support of this research. The NIH supplemental awards 3R01GM118510-03S1 and 3R01GM087605-06S1 as well as the Vagelos Institute for Energy Science and Technology supported the purchase of the NMR instrumentation used in this study.

REFERENCES

1. Yan, N.-H.; Luo, H., Transition metal mediated activation of C(sp^3)–C(sp^2) bond in aromatic hydrocarbons. *Synth. Commun.* **2021**, 1-18.
2. Bandyopadhyay, A.; Basak, G. C., Studies on photocatalytic degradation of polystyrene. *Mater. Sci. Technol.* **2007,** *23* (3), 307-314.
3. Murakami, M.; Ishida, N., Potential of Metal-Catalyzed C–C Single Bond Cleavage for Organic Synthesis. *J. Am. Chem. Soc.* **2016,** *138* (42), 13759-13769.
4. Jun, C.-H., Transition metal-catalyzed carbon–carbon bond activation. *Chem. Soc. Rev.* **2004,** *33* (9), 610-618.
5. Kondo, T.; Nakamura, A.; Okada, T.; Suzuki, N.; Wada, K.; Mitsudo, T.-a., Ruthenium-Catalyzed Reconstructive Synthesis of Cyclopentenones by Unusual Coupling of Cyclobutenediones with Alkenes Involving Carbon−Carbon Bond Cleavage. *J. Am. Chem. Soc.* **2000,** *122* (26), 6319-6320.
6. Song, F.; Gou, T.; Wang, B.-Q.; Shi, Z.-J., Catalytic activations of unstrained C–C bond involving organometallic intermediates. *Chem. Soc. Rev.* **2018,** *47* (18), 7078-7115.
7. Aoki, S.; Fujimura, T.; Nakamura, E.; Kuwajima, I., Palladium-catalyzed arylation of siloxycyclopropanes with aryl triflates. Carbon chain elongation via catalytic carbon-carbon bond cleavage. *J. Am. Chem. Soc.* **1988,** *110* (10), 3296-3298.
8. Fumagalli, G.; Stanton, S.; Bower, J. F., Recent Methodologies That Exploit C–C Single-Bond Cleavage of Strained Ring Systems by Transition Metal Complexes. *Chem. Rev.* **2017,** *117* (13), 9404-9432.
9. Vicente, R., C–C Bond Cleavages of Cyclopropenes: Operating for Selective Ring-Opening Reactions. *Chem. Rev.* **2021,** *121* (1), 162-226.
10. Cohen, Y.; Cohen, A.; Marek, I., Creating Stereocenters within Acyclic Systems by C–C Bond Cleavage of Cyclopropanes. *Chem. Rev.* **2021,** *121* (1), 140-161.
11. Chen, P.-h.; Billett, B. A.; Tsukamoto, T.; Dong, G., "Cut and Sew" Transformations via Transition-Metal-Catalyzed Carbon–Carbon Bond Activation. *ACS Catal.* **2017,** *7* (2), 1340-1360.
12. Periana, R. A.; Bergman, R. G., Carbon-carbon activation of organic small ring compounds by arrangement of cycloalkylhydridorhodium complexes to rhodacycloalkanes. Synthesis of metallacyclobutanes, including one with a tertiary metal-carbon bond, by nucleophilic addition to π-allyl complexes. *J. Am. Chem. Soc.* **1986,** *108* (23), 7346-7355.
13. Leforestier, B.; Gyton, M. R.; Chaplin, A. B., Oxidative Addition of a Mechanically Entrapped C(*sp*)–C(*sp*) Bond to a Rhodium(I) Pincer Complex. *Angew. Chem. Int. Ed.* **2020,** *59* (52), 23500-23504.
14. Dewhurst, R. D.; Hill, A. F.; Rae, A. D.; Willis, A. C., Reactions of Bis(tricarbido)mercurials and Dimetallaoctatetraynes with $[Ru(CO)_2(PPh_3)_3]$: Scission of a C*sp*−C*sp* Single Bond. *Organometallics* **2005,** *24* (20), 4703-4706.
15. Müller, C.; Iverson, C. N.; Lachicotte, R. J.; Jones, W. D., Carbon−Carbon Bond Activation in Pt(0)−Diphenylacetylene

Complexes Bearing Chelating P,N- and P,P-Ligands. *J. Am. Chem. Soc.* **2001,** *123* (39), 9718-9719.
16. Li, T.; Wang, Z.; Zhang, M.; Zhang, H.-J.; Wen, T.-B., Rh/Cu-catalyzed multiple C–H, C–C, and C–N bond cleavage: facile synthesis of pyrido[2,1-a]indoles from 1-(pyridin-2-yl)-1H-indoles and γ-substituted propargyl alcohols. *Chem. Commun.* **2015,** *51* (31), 6777-6780.
17. Qin, C.; Feng, P.; Ou, Y.; Shen, T.; Wang, T.; Jiao, N., Selective C_{sp2}−C_{sp} Bond Cleavage: The Nitrogenation of Alkynes to Amides. *Angew. Chem. Int. Ed.* **2013,** *52* (30), 7850-7854.
18. Suzuki, A.; Wu, L.; Lin, Z.; Yamashita, M., Isomerization of a cis-(2-Borylalkenyl)Gold Complex via a Retro-1,2-Metalate Shift: Cleavage of a C−C/C−Si Bond trans to a C−Au Bond. *Angew. Chem. Int. Ed.* **2021,** *60* (38), 21007-21013.
19. Weisheit, T.; Escudero, D.; Petzold, H.; Görls, H.; González, L.; Weigand, W., Photochemical behavior of (diphosphine)(η^2-tolane)Pt^0 complexes. Part A: Experimental considerations in solution and in the solid state. *Dalton Trans* **2010,** *39* (40), 9493-9504.
20. Gunay, A.; Müller, C.; Lachicotte, R. J.; Brennessel, W. W.; Jones, W. D., Reactivity Differences of Pt0 Phosphine Complexes in C−C Bond Activation of Asymmetric Acetylenes. *Organometallics* **2009,** *28* (22), 6524-6530.
21. Anderson, G. K.; Lumetta, G. J.; Siria, J. W., Photochemical reactions of diphosphineplatinum(II) oxalate complexes. *J. Organomet. Chem.* **1992,** *434* (2), 253-259.
22. Gunay, A.; Brennessel, W. W.; Jones, W. D., Investigation of C–C Bond Activation of *sp–sp*^{2} C–C Bonds of Acetylene Derivatives via Photolysis of Pt Complexes. *Organometallics* **2015,** *34* (11), 2233-2239.
23. Escudero, D.; Weisheit, T.; Weigand, W.; González, L., Photochemical behavior of (bisphosphane)(η^2-tolane)Pt^0 complexes. Part B: An insight from DFT calculations. *Dalton Trans* **2010,** *39*, 9505-9513.
24. Liu, T.; Gau, M. R.; Tomson, N. C., Mimicking the Constrained Geometry of a Nitrogen-Fixation Intermediate. *J. Am. Chem. Soc.* **2020,** *142* (18), 8142-8146.
25. The Δ parameter is an empirical metric used to describe the physical oxidation states of PDI ligands based on characteristic bond lengths of the ligand backbone. We recently adapted it into the units suitable for $^3PDI_2$.
26. Römelt, C.; Weyhermüller, T.; Wieghardt, K., Structural characteristics of redox-active pyridine-1,6-diimine complexes: Electronic structures and ligand oxidation levels. C*oord. Chem. Rev.* **2019,** *380,* 287-317.
27. Darmon, J. M.; Stieber, S. C. E.; Sylvester, K. T.; Fernández, I.; Lobkovsky, E.; Semproni, S. P.; Bill, E.; Wieghardt, K.; DeBeer, S.; Chirik, P. J., Oxidative Addition of Carbon–Carbon Bonds with a Redox-Active Bis(imino)pyridine Iron Complex. *J. Am. Chem. Soc.* **2012,** *134 (*41), 17125-17137.
28. A species related to the proposed intermediate **B'** is not observed experimentally. We attribute the quantitative inaccuracy of our computational model to the truncation of PMe_3 for PPh_3, as doing so presents less steric repulsion towards the alkynyl group within **B'** than what would be present in the untruncated structure.